Pressure Fluctuations Induced by Road Vehicles in Ambient Air - A Model Study –

I. U. Macciacchera[1] **& B. Ruck**[2]
[1] *Dipartamento n. 37, Idraulica, Trasporti e Strade, Universitá 'La Sapienza', Rome, Italy*
[2]*Laboratory of Building and Environmental Aerodynamics, Institute for Hydromechanics (IfH), University of Karlsruhe, Germany*

Abstract

In urban areas, car exhausts play a significant role in the overall pollutant budget. Pollutant dispersion in urban structures is believed to be influenced by car-induced turbulent diffusion. To assess this influence, it is most important to attain a thorough knowledge of the fluid mechanics involved. There are two problems associated with this problem. First of all, the physical phenomenon itself must be identified clearly, and secondly, an adequate modelling technique must be realized for the physical modelling in simulation studies such as wind tunnel investigations.
To contribute to the fundamental understanding of car-induced turbulent mixing in the ambient air, a model study was carried out in order to measure the car-induced pressure disturbation field in direct vicinity of the street. The points of measurement were placed at various distances from the street as to discretize the decaying influence of the disturbation. The measurements were performed with various car models differing in shape.
The experimental study was carried out with moving car models in 1:30 scale passing through a frame of adjacent pressure tapings. The height and width of the frame was varied in order to simulate the influence of varying distance from the car. The pressure field was measured time-dependently. The individual car was measured many times with the same speed in order to achieve a comprehensive impression of the transient 3-D pressure field disturbation. Differing from usual wind tunnel studies, the cars investigated were moved over the ground, accounting also for boundary layer effects of e.g. rotating wheels.

1 Scale models considerations

Many tests have been performed on scale models to understand transport and shape modification of roads vehicles ([11], [10]). The transferability of model tests to full scale is uncertain. As can be deduced it is not possible to reproduce the same Reynolds number and the correspondent Mach number in the same time. Also the energy production can changes in model and in full scale. A possible way is to increase velocity in the model wind tunnel below the critical Mach number ($Ma<0.2$) ([4], [2], [3]). The influence of Reynolds number is small for $Re>10^7$ for several body shapes.
When there are effects of external wind and interactions with others vehicles, the ratio between energy production from vehicles drag and external wind must be the same in model and in reality [6].
The Reynolds number is $\mathrm{Re} = \frac{v \cdot l}{\nu}$ where v is the velocity of the car, l denotes a characteristic length (fig.1) and ν the dynamic viscosity of air.

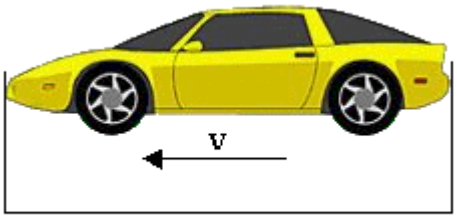

$$Fd = C_w \frac{\rho \cdot v^2}{2} A$$

Fig. 1 – A generic vehicle and the characteristic length l.

To obtain $Re_m = Re_n$ (the index m stands for model and the index n for full size conditions), it should be:

$$\frac{v_m \cdot l_m}{\nu} = \frac{v_n \cdot l_n}{\nu}; \; v_m \cdot \left(\frac{l_n}{M}\right) = v_n \cdot l_n; \; v_m = M \cdot v_n \tag{1}$$

Where M is a scale between the model and the real condition.

The Mach number is $Ma = \frac{v}{v_s}$, where v_s is the velocity of sound, and to obtain $Ma_m = Ma_n$ it should be:

$$\frac{v_m}{v_s} = \frac{v_n}{v_s};$$

$$v_m = v_n \tag{2}$$

The drag energy is $E = C_w \frac{\rho \cdot v^3}{2} A$, where ρ is the density of air, A the frontal Area of the vehicle and C_w the drag coefficient. To obtain $E_m = E_n$ it should be:

$$C_w \frac{\rho \cdot v_m^{\,3}}{2} A_m = C_w \frac{\rho \cdot v_n^{\,3}}{2} A_n; \qquad v_m^{\,3} \cdot A_m = v_n^{\,3} \cdot A_n; \; v_m^{\,3} \frac{A_p}{M^2} = v_n^{\,3} \cdot A_m;$$

$$v_m = M^{\frac{2}{3}} \cdot v_n \tag{3}$$

When there is traffic and wind, Plate [6] based the modelling criteria on the condition that the ratio of energy production P_T caused by moving traffic to the energy production P_W caused by the wind should be the same in the model and in the real condition:

$$\frac{P_{tm}}{P_{wm}} = \frac{P_{tn}}{P_{wn}} = T_t; \tag{4}$$

Where:

$$P_t = \frac{\rho \cdot C_w \cdot A \cdot n_t \cdot v^3}{B \cdot H}; \tag{5}$$

and

$$P_w = \tau \frac{\Delta u}{\Delta z} \approx \frac{\rho \cdot u_*^{\,2}}{H} u(H) \propto \frac{\rho \cdot c_{fh} \cdot u^3}{H}; \qquad u_* = \sqrt{c_{fh}} \cdot u; \tag{6}$$

Where H is the street canyon height, B the street canyon width (fig.2), τ the shear stress, c_{fh} the friction coefficient , u_* the shear velocity, n the number of vehicles per unit length.

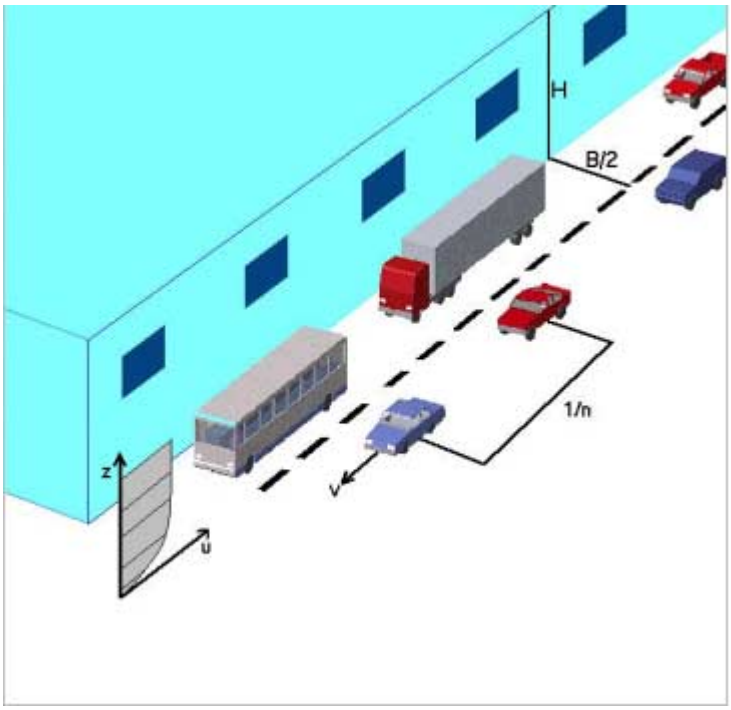

Fig.2 – Traffic and wind in a city street.

Introducing equation (5) and (6) in (4) yeld:

$$T_t = \frac{C_w \cdot A \cdot n_t}{c_{fh} \cdot B} \cdot \frac{v^3}{u^3}; \qquad \frac{C_w \cdot A_m \cdot n_{tm}}{c_{fh} \cdot B_m} \cdot \frac{v_m^{\,3}}{u_m^{\,3}} = \frac{C_w \cdot A_n \cdot n_{tn}}{c_{fh} \cdot B_n} \cdot \frac{v_n^{\,3}}{u_n^{\,3}}; \tag{7}$$

$$\frac{A_n}{M^2} \cdot n_{tm} \cdot \frac{M}{B_n} \cdot \frac{v_m^{\,3}}{u_m^{\,3}} = \frac{A_n \cdot n_{tn}}{B_n} \cdot \frac{v_n^{\,3}}{u_n^{\,3}}; \qquad \frac{\left(\frac{v_n^{\,3}}{u_n^{\,3}}\right)}{\left(\frac{v_m^{\,3}}{u_m^{\,3}}\right)} = \frac{n_{tm}}{n_{tn}} = a; \qquad \left(\frac{v_n}{u_n}\right)^3 = \left(\frac{v_m}{u_m}\right)^3 \cdot a; \tag{8}$$

$$\frac{v_n}{u_n} = a^{(1/3)} \cdot \frac{v_m}{u_m}. \tag{9}$$

It is no doubt that experiments in full scale [1,7] are the best way to obtain reliable values. However, equ.(9) shows that in the laboratory realistics (energetical) conditions can be realized. This theory [6] is based only on energetical conditions and does not account for the specific kind of turbulence production. As a matter of fact, many laboratory experiments were carried out with model cars [5,8 and 9] showing a different shape as real cars. The question arises, however, how the results can be transferred to nature. Therefore experiments with model cars of simple geometry were carried out in order to assens the disturbation fields in the ambient air. This allows later the comparison of the results with real measurements.

2 Experimental Setup

The laboratory model of the test loop is shown in fig.3.

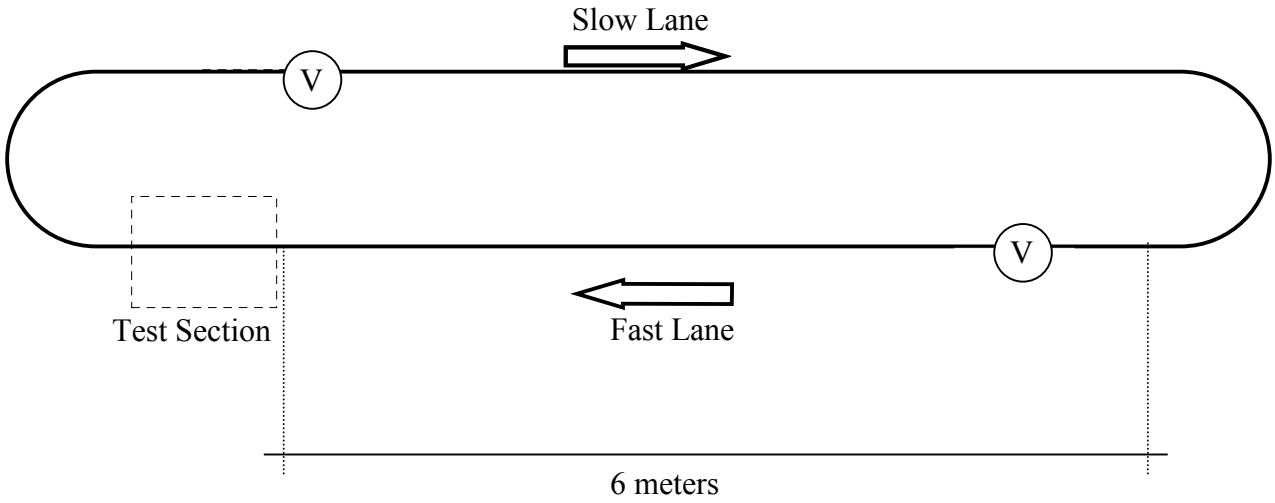

Fig.3 – Experimental setup.

It is realized one plastic street of 20 cm width (1:30 scale), and therefore, represents a real street of 6 m width. The street is divided in two carriageways and a generic vehicle can circulate getting power from electric contacts located in the middle of each carriageway . The closed circuit is separated in two parts , everyone is fed from different voltages. The first part represent the fast lane where the measurements are taken. The second part is the slow lane where the model cars go back to the start position of the fast lane.
The measurements of pressure are taken by a system of a piezoresistive pressure transducer (Endvco series 8507 B with diameter of 0,9 millimetres) and a differential amplifier (PSC 8015-1). The velocity of the vehicle model is obtained from two consecutive contacts positioned in a known distance (Fig. 4).

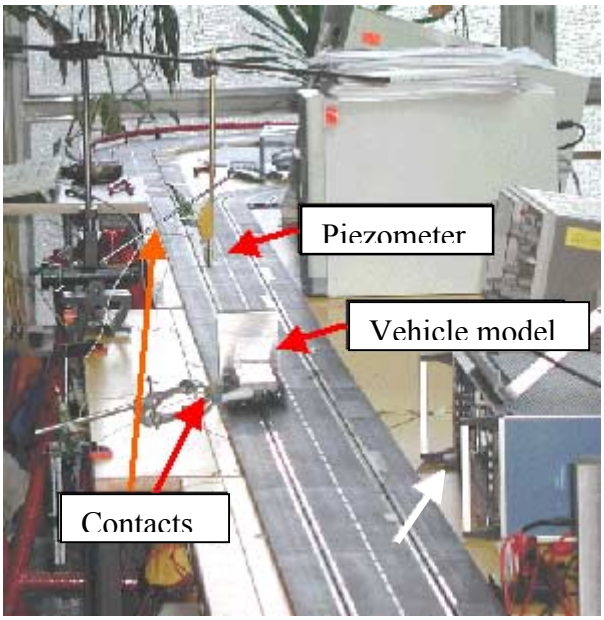

Fig. 4 – A photo of the experimental setup.

3 Results

In this study there were analyzed two model with different shapes.
The first model analyzed has a simple plate in the frontal as shown in fig.5.

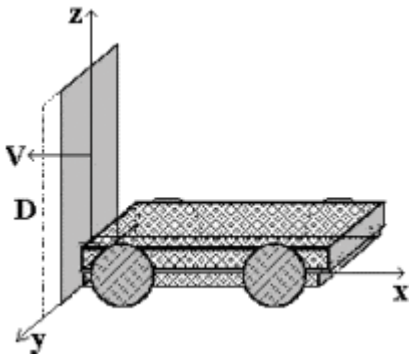

Fig.5 – Sketch of model with plate in the frontal part and system of reference.

As usual, the x-axes is opposite to the movement direction, the y-axes horizontal, normal to the movement direction and z is the vertical axes. The velocity of the model is v. The characteristic length is D, the height of the plate.
The frontal area at the model is typical for transport vehicles e.g. trucks (fig.6).

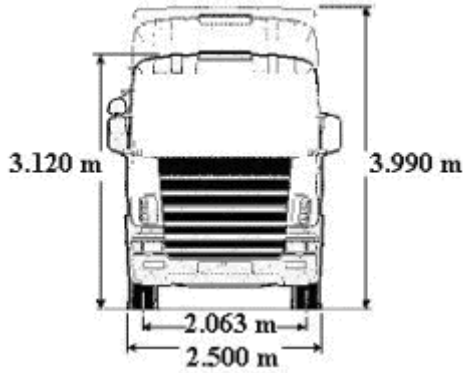

Fig.6 – Dimensions of a frontal surface of a typical transport vehicle.

The scale of the model is 1:30 and the dimensions of the street and the frontal surface of the model are shown in the table below:

	Street Width [m]	H, Camion Width [m]	D, Camion Height [m]
In Reality	3.00	2.50	3.10
In Model	0.10	0.08	0.10

The velocity of the model have been fixed during the measurements to the value of 4.7 m/s and a Reynolds number of 32500 was realized.
The pressure is expressed by the dimensionless coefficient Cp:

$$C_p = \frac{p - p_\infty}{\rho \cdot v^2 / 2g};$$

Where p is the dynamic pressure and p_∞ the static pressure.

The term $\rho \cdot v^2 / 2g$ had a value of 13.3 Pascal.

The experimental setup did not permit to investigate the field of Cp in the place taken from the vehicle model during the passing of the street and the place very close to the vehicle model

(y/D<0.5 and z/D<1.1); the resolution of measurements is 0.5 cm (0.05*D) in x-direction and 1 cm (0.1*D) in y- and z-directions.
In figure 7,8 and 9 there are shown tree Cp field sections x-y for different z.

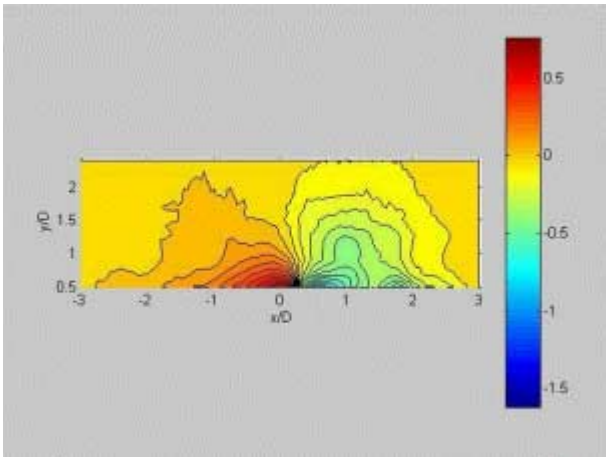

Fig.7 – Section xy of Cp field for z/D=0.

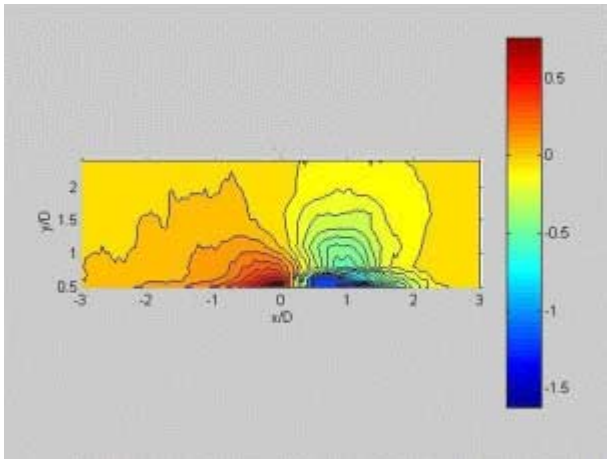

Fig.8 – Section xy of Cp field for z/D=0.5.

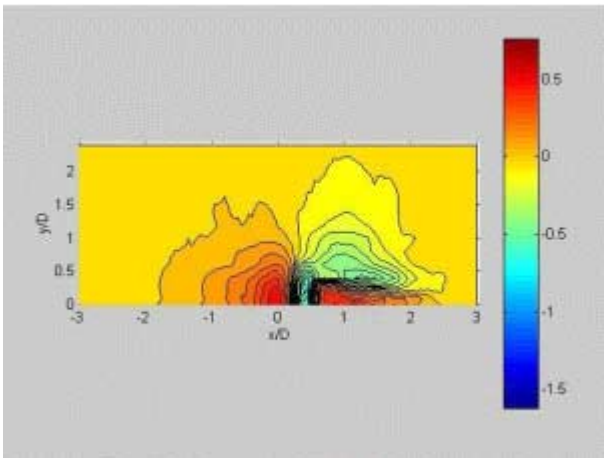

Fig.9 – Section xy of Cp field for z/D=1.1.

At the lateral side, the field of pressure is positive in correspondence to the frontal surface of the vehicle model. Behind the vehicle, the pressure becomes negative.
The pressure is also positive for x/D<0.
The distribution of the field of Cp in the sections z/D=0 (fig.7) and in the section z/D=0.5 is similar (fig.8), but in the section z/D=1.1 (fig.9) we can observe a zone on the upper side of the vehicle where the pressure is positive also for x/D>0 and this zone is separate from the first zone of positive pressure (in correspondence to the frontal surface) by a little zone where the pressure is negative. We can observe the profile of pressure along the x direction at different y-positions (z/D=0, Fig.10 and z/D= 0.5, Fig.11).
The results show that Cp has the maximum value at the middle of the frontal surface (z/D=0.5 and y/D=0.5) where with x/D=0 Cp, has a value of 0.8 and with x/D=0.4, Cp has a value of –1.6, the double in absolute value with respect to the maximum of the positive value.
On the uppper side, the situation changes because the shape of the model induces an air flow in upward direction (z) and the pressure is also positive after the vehicle passing, as can be observed in the graphics below, where the profiles of pressure are traced along the x-axis for different z-positions (where z/D>1) with y/D= 0 (Fig.12).

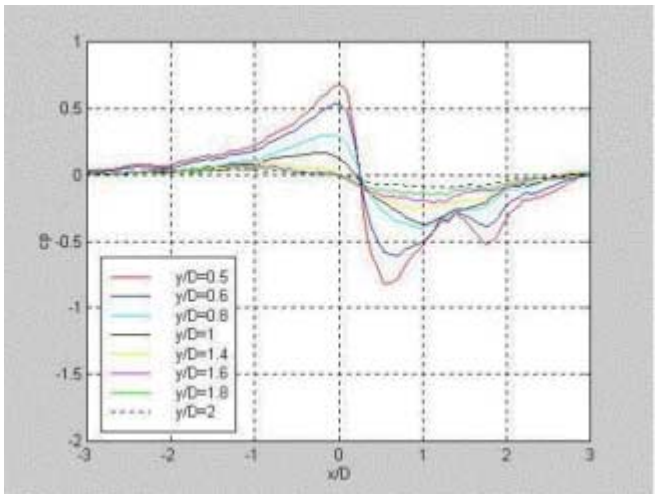

Fig.10 – Profiles of pressure along x direction for z/D=0.

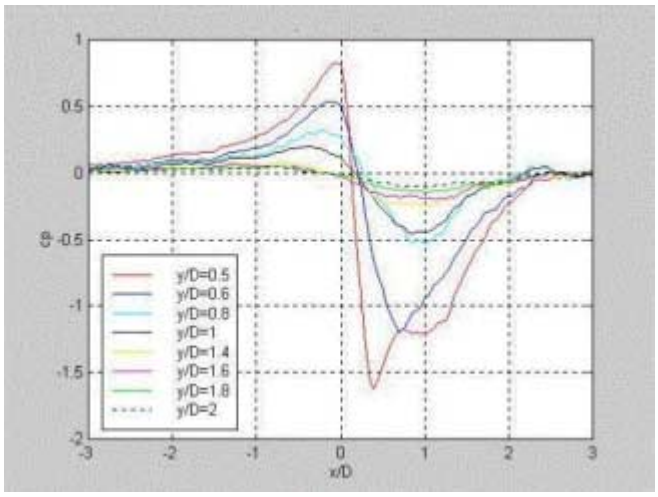

Fig.11 – Profiles of pressure along x direction for z/D=0.5.

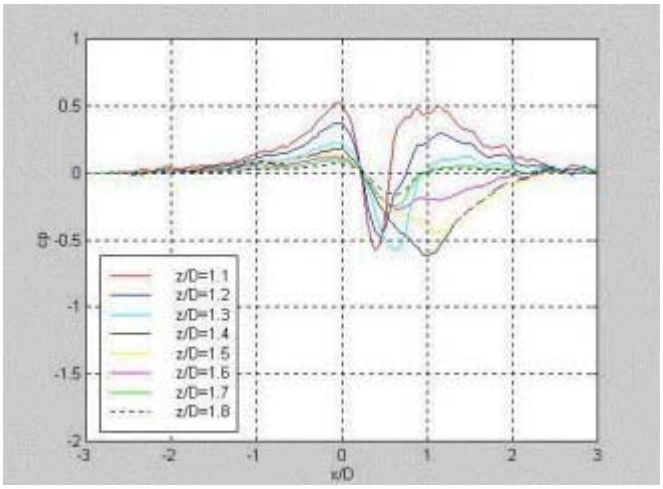

fig.12 – Profiles of pressure along x direction for y/D=0.

Below there are shown two x-z sections and we can observe in detail how the distribution of pressure on the upper side remains positive in correspondence to the frontal surface of the vehicle model. It is also positive for y/D>0 (fig 13).

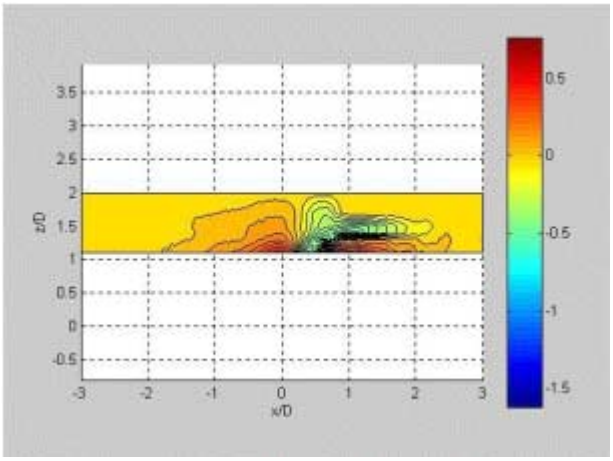

Fig.13 – Section xz of Cp field for y/D=0.

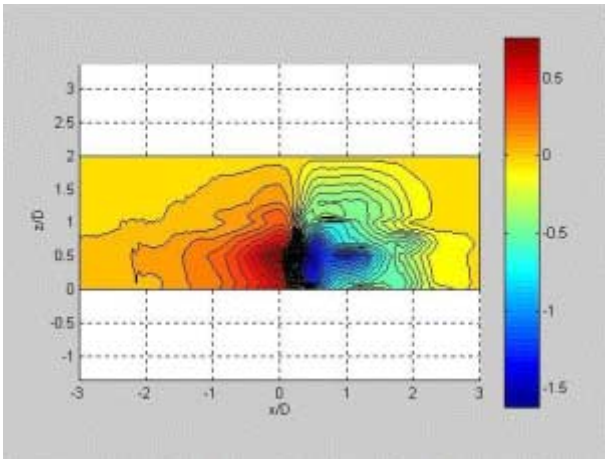

Fig.14 – Section xz of Cp field for y/D=0.5.

This fact is important with respect to the distribution of pollutants induced by vehicle movement. In figure 14, the section of the field of Cp for y/D=0.5 is shown. It can be seen, how the pressure increases before the frontal surface and decreases for x/D>0 for all zones z/D<1. In the lateral side the zone where the pressure is negative is more larger than the zone where the pressure is positive, for a fixed absolute value of Cp.
To have a complete image of the pressure field there are shown zy-sections of the field of Cp for x/D=0 (fig.15) for x/D=0.6 (fig.16) and for x/D=1 (fig.17) and the corrisponding graphs of Cp in the y-direction for different x-positions (fig.18 , fig 19 and fig.20) and z direction (fig.21, fig 22 and fig.23).

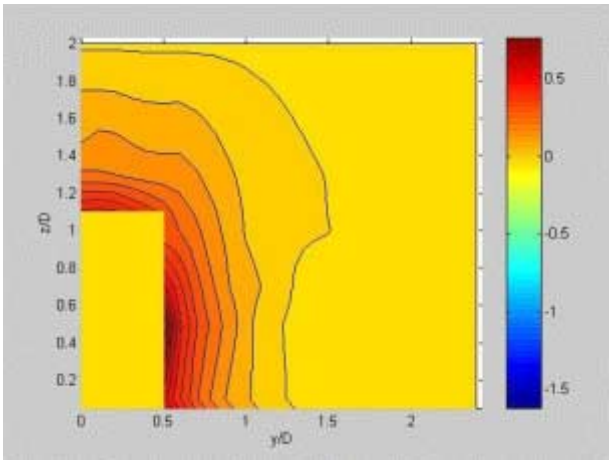

Fig.15 – Section yz of Cp field for x/D=0.

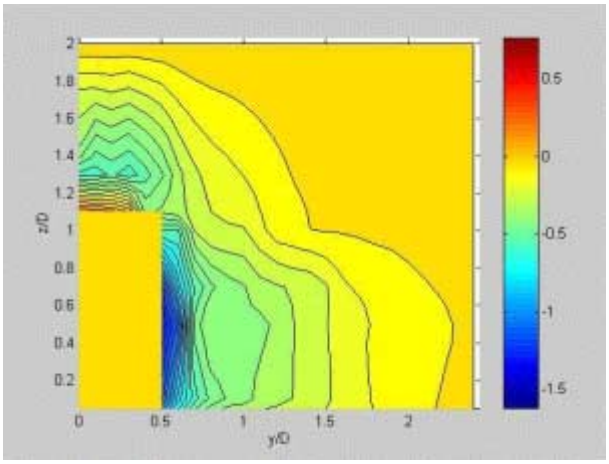

Fig.16 – Section yz of Cp field for x/D=0.6.

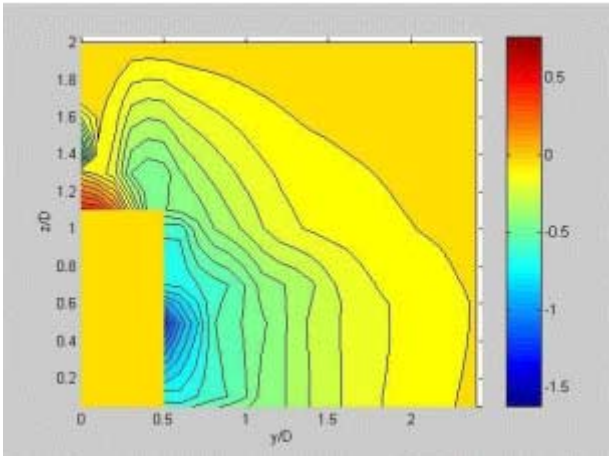

Fig.17 – Section yz of Cp field for x/D=1.

The field of Cp at the frontal surface is shown in figure 15 and in the y-direction (fig.18) the pressure influence of the vehicle is not more than 1.5*D. In figure 21 we can observe how, in lateral direction, the pressure increases from the ground to the middle of the frontal surface and afterwards decreases until z/D=2. For x/D=0.6, the pressure on the upper side decreases (fig.16, 19 and 22) and there is a zone of negative pressure. For x/D=1 (fig17, 20 and 23) there is a new increase. At the lateral side, for the section x/D=0.6, the pressure becomes negative and it has the maximum value of negative pressure (-1.6, fig.22) close to the vehicle model (y/D=0.5). The effect in space of the vehicle passing extents until y/D=2 (fig.19). Nearly the same situation cn be found, for the lateral-side, where in the section for x/D=1 (fig.17) the negative pressure shows a minor value than in x/D=0.6.

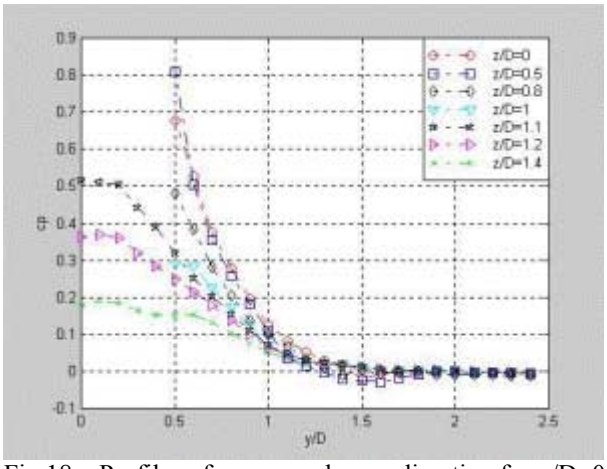

Fig.18 – Profiles of pressure along y direction for x/D=0.

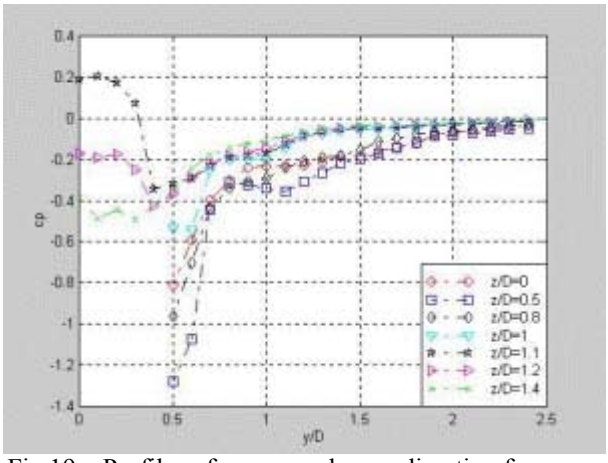

Fig.19 – Profiles of pressure along y direction for x/D=0.6.

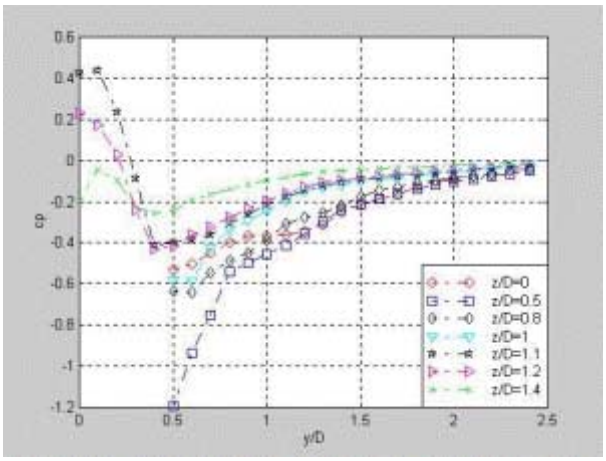

Fig.20 – Profiles of pressure along y direction for x/D=1.

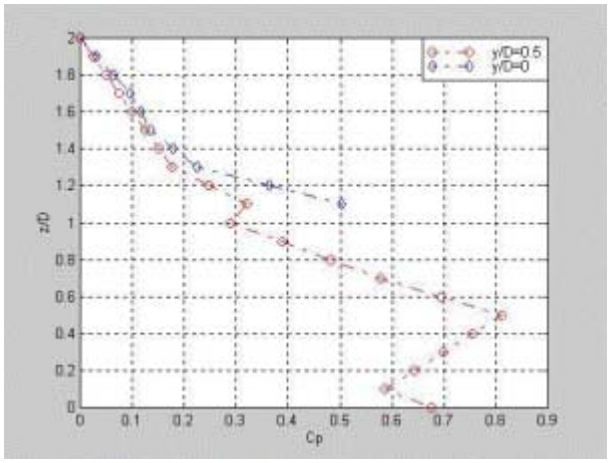

Fig.21 – Profiles of pressure along z direction for x/D=0

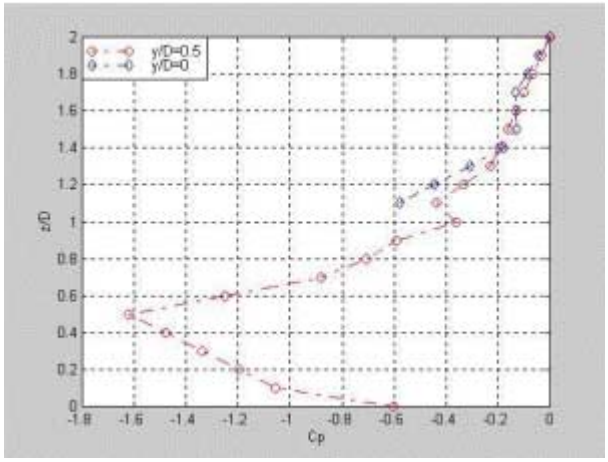

Fig.22 – Profiles of pressure along z direction for x/D=0.6.

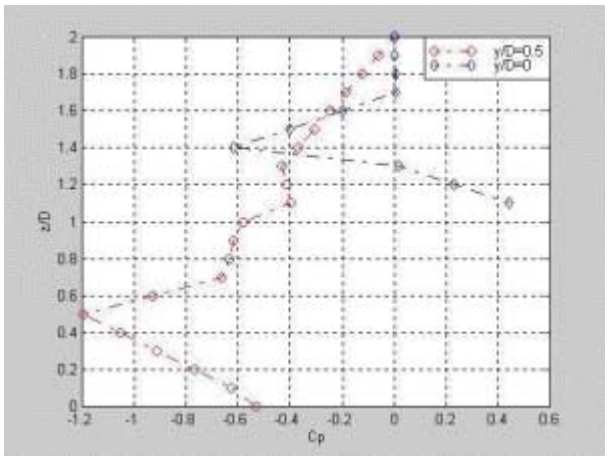

Fig.23 – Profiles of pressure along z direction for x/D=1.

The situation becomes different changing the the vehicle model shape.
The second model analyzed has a geometry of a rectangular block. The size of the frontal part is the same as of the plate model.
The sketch of this model is shown in fig.24.
The characteristic length is D (the height of the block), the horizontal length is L. About the characteristic length L of a typical transport vehicle, see figure 25.

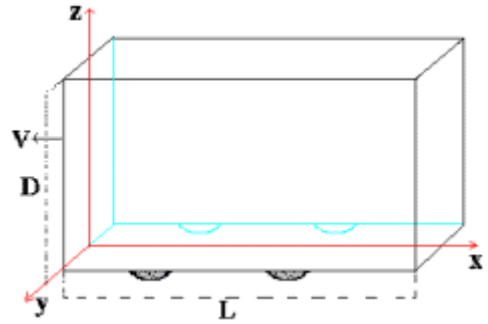

Fig.24 – Sketch of rectangular block model and system of reference.

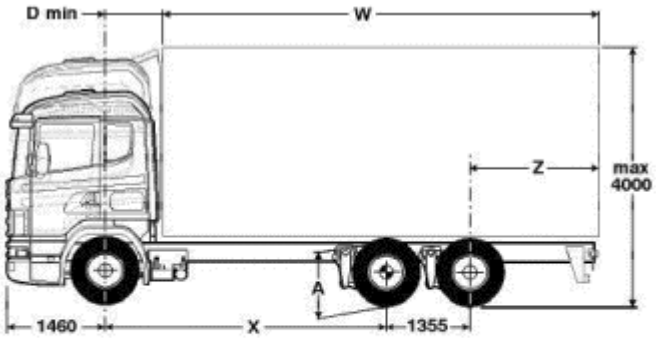

X		3.900	4.100	4.300	4.500	4.700	4.900	5.100	5.300	5.500	5.900
W	max	6.183	6.513	6.872	7.232	7.601	7.964	8.331	8.759	9.059	9.655
W	min	5.971	6.200	6.642	6.991	7.351	7.704	8.061	8.490	8.847	9.572
Z	max	1.813	1.943	2.102	2.262	2.431	2.594	2.761	2.989	3.089	3.285
Z	min	1.601	1.630	1.872	2.021	2.181	2.334	2.491	2.720	2.877	3.202

Fig.25 – Parameters about the determination of the length of a transport vehicle (The dimensions are in millimeters).

The figure 26 shows the heigth and the length of several transport vehicles.
Typical widths are 2.5 m.

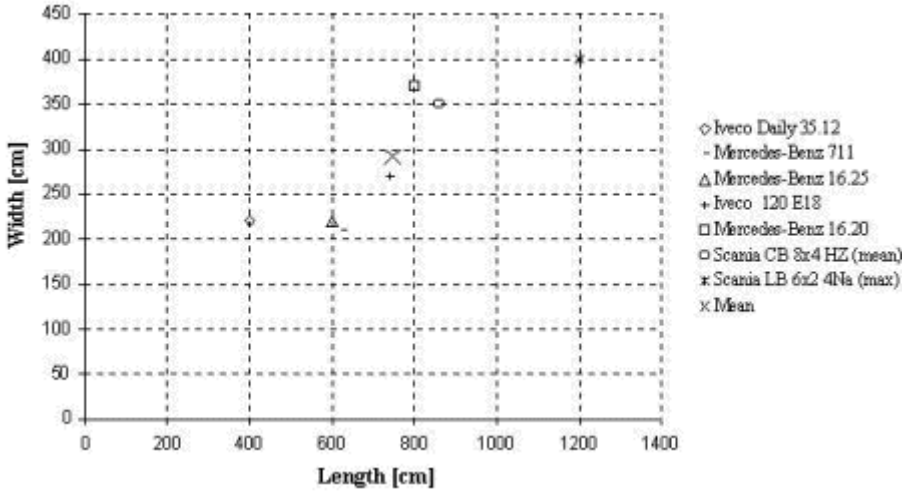

fig.26 – Height and length of several transport vehicles and determination of the mean.

The scale of the model is 1:30 and the dimensions of the street and the model are shown in the table below:

	Street Width [m]	H, Vehicle Width [m]	D, Vehicle Height [m]	L, Camion Length [m]
In Reality	3.00	2.50	3.10	7.44
In Model	0.10	0.08	0.10	0.24

The velocity of the model have been fixed during the measurements to the value of 4 m/s and a Reynolds number Re_D of 27600 and Re_L of 64000 was realized. The term $\rho \cdot v^2/2g$ had a value of 9.6 Pascal.
In figure 27 there is shown the secton x-y for Cp field for z/D=0.5 and in figure 28 the corrisponding graph.

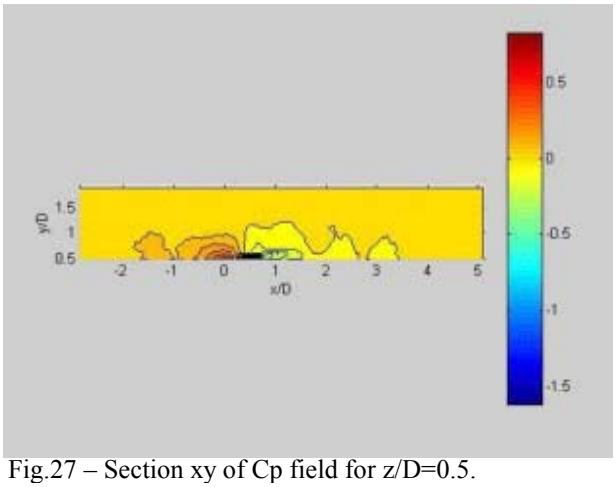

Fig.27 – Section xy of Cp field for z/D=0.5.

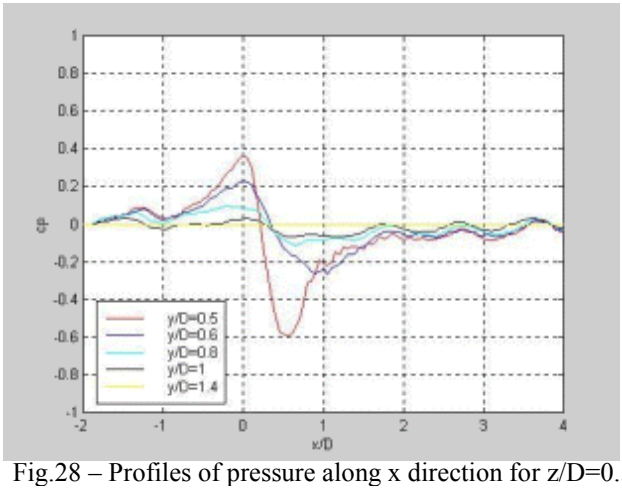

Fig.28 – Profiles of pressure along x direction for z/D=0.5.

Also for this model, like the plate model, in lateral direction, the pressure increases until x/D=0 and the pressure becomes negatve for x/D>0 (Fig.28).
In figure 29 there is the xz section of Cp for y/D=0.5. In figure 30 the zy section in x/D=0.

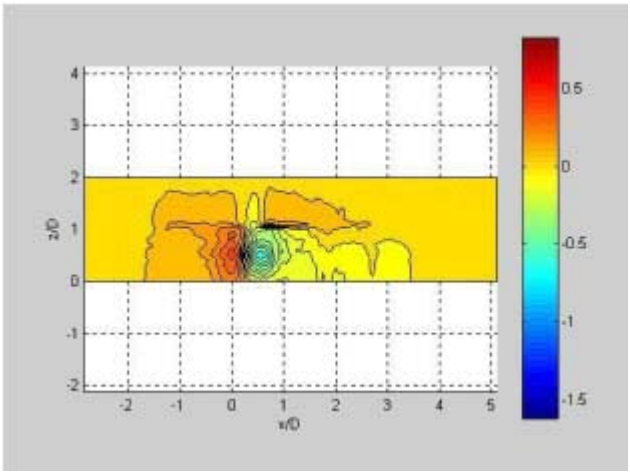

Fig.29 – Section xz of Cp field for y/D=0.5.

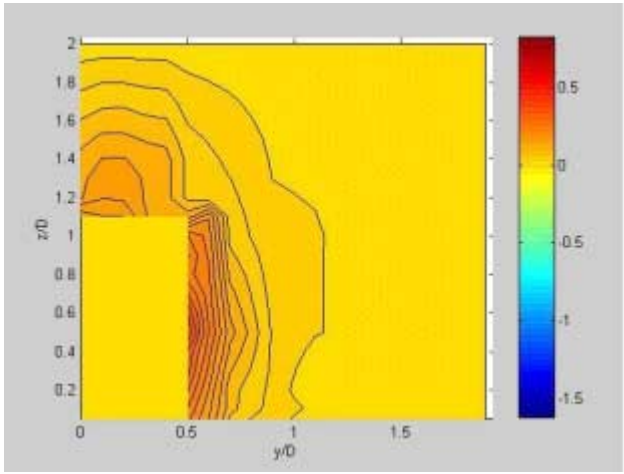

Fig.30 – Section yz of Cp field for x/D=0.

The corrisponding graphs are shown in figures 31 and 32.

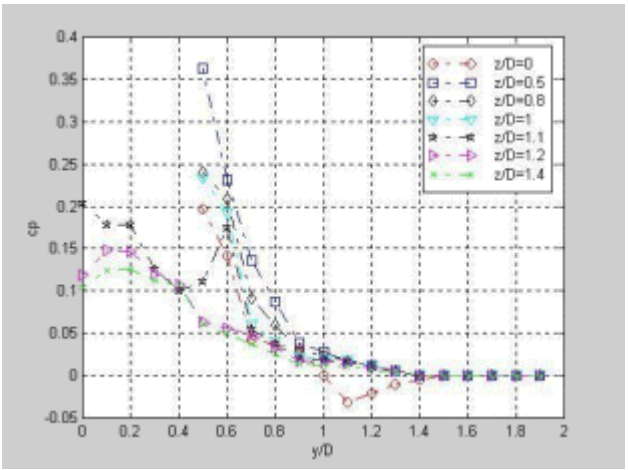

Fig.31 – Profiles of pressure along y direction for x/D=0.

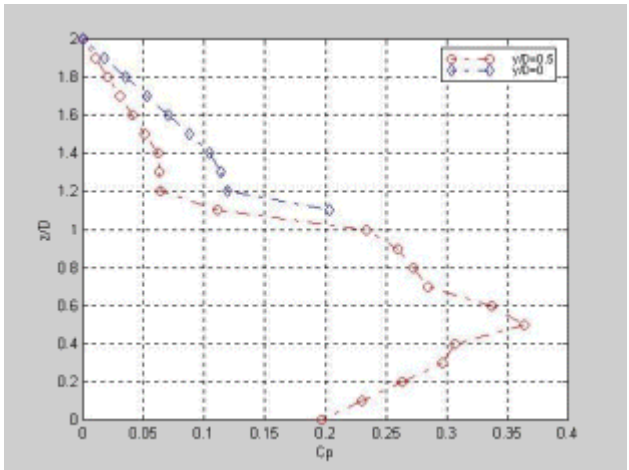

Fig.32 – Profiles of pressure along z direction for x/D=0

A comparison of the results of the two different models shows that the absolute value of pressure differs; however the form of the pressure distributions is similar. The plate model extens a greater influence in the ambient around in lateral direction whereas in the direction of movement the block model shows greater disturbances.

4 Acknowledgement

The authors would like to thank the European Commission for the funding of this study within the frame project TRAPOS.

References

[1] Filoni S., Indagine sperimentale con sonda a 5 fori e anemometro a filo caldo di correnti separate prodotte su autoveicoli da elementi esterni ,Tesi di laurea in ingegneria Aeronautica, dipartimento di Scienza ed Ingegneria dello Spazio, Napoli, 2000.

[2] Genta G., Meccanica dell'Autoveicolo ,Levrotto & Bella, Torino, 1989.

[3] Gillespie T. D., Fundamentals of vehicle dynamics. ,SAE, 1992.

[4] Hucho W. H., Aerodynamics of Road Vehicles Edition:4, Butterworths, London,1998.

[5] Kastner-Klein, Berkovicz, Rastetter A., Plate E.J., Modelling of nVehicle Induced Turbulence in Air Pollution Studies for Streets, 5th International Conference on Harmonisatin within Atmospheric Dispersion Modelling for Regulatory Purposes, Rhodes, Greece, 1998.

[6] Plate E.J., Windkanalmodellierung von Ausbreitungsvorgangen in Stadtgebieten, Verlag TUV Rheinland,1982.

[7] Pope, A, Rae W.H., Low-Speed Wind Tunnel Testing, John Wiley, New York, 1984.

[8] Shaw C.T, Garry K.P., Gress T., Using singular systems analysis to characterise the flow in the wake of a model passenger vehicle, Journal of Wind Engineering and Industrial Aerodynamics N85, pp.1-30, 2000.

[9] SHIEHLEN W. O., Modelling complex vehicle systems.,Proc. 8th IAVSD Symp on dynamics of vehicles on roads and on railway tracks, Cambridge MA,pp. 548-563, 1983.

[10] Sighard F., Fluid –Dynamic drag ,Hoerner, 1965.

[11] Sovran G, Morel T, Mason, Aerodynamic Drag Mechanisms of Bluff Bodies and RoadVehicles, Plenum Press, New York,1978.